Received: 26 July 2024 | Revised: 3 September 2024 | Accepted: 9 September 2024

DOI: 10.1002/cm.21933

RESEARCH ARTICLE

CYTOSKELETON WILEY

F-actin in the cuticular plate and junctions of auditory hair cells is regulated by ADF and cofilin to allow for normal stereocilia bundle patterning and maintenance

Jamis McGrath | **Katelin Hawbaker** | **Benjamin J. Perrin**

Department of Biology, Indiana University – Indianapolis, Indianapolis, Indiana, USA

Correspondence
Benjamin Perrin, Department of Biology, Indiana University – Indianapolis, 723 W. Michigan St, Indianapolis IN 46202, USA.
Email: bperrin@iu.edu

Funding information
National Institutes of Health

Abstract

Auditory hair cells, which convert sound-induced vibrations in the inner ear into neural signals, depend on multiple actin populations for normal function. Stereocilia are mechanosensory protrusions formed around a core of linear, crosslinked F-actin. They are anchored in the cuticular plate, which predominantly consists of randomly oriented actin filaments. A third actin population is found near hair cell junctions, consisting of both parallel and branched filaments. Actin depolymerizing factor (ADF) and cofilin-1 (CFL1) proteins disassemble actin filaments and are required to regulate F-actin in stereocilia, but their effect on cuticular plate and junctional actin populations is unclear. Here, we show that loss of ADF and CFL1 disrupts the patterning of stereocilia into orderly bundles and that this phenotype correlates with defective development of the cuticular plate and junctional actin populations. ADF/CFL1 continue to regulate these actin populations in mature cells, which is necessary for long-term maintenance of hair cell morphology.

KEYWORDS
actin, cofilin, morphogenesis, stereocilia

1 | INTRODUCTION

Sound is detected in the mammalian inner ear by two types of auditory hair cells which are precisely arranged along the length of the organ of Corti. A single row of inner hair cells (IHCs) is located medial to three rows of outer hair cells (OHCs; Figure 1a). Each hair cell has a well-organized V-shaped bundle of actin-based protrusions called stereocilia. The bundles are oriented such that their vertices point toward the lateral edge of the tissue. Bundles are deflected along the mediolateral axis by sound-induced vibrations to initiate mechanotransduction and auditory perception. Thus, forming stereocilia that are patterned into properly arranged bundles is important for auditory sensitivity.

Individual stereocilia are largely made up of a core of parallel, crosslinked actin filaments. A dense F-actin rootlet extends from stereocilia into a gel-like network of randomly oriented actin filaments at the cell apex, called the cuticular plate (Tilney et al., 1980). Filaments in the cuticular plate are loosely packed and interlinked by F-actin binding proteins including αII- and βII-spectrins, plastin, xin-interacting repeat protein 2 (XIRP2), supervillin (SVIL), and LIM only protein 7 (LMO7) (Du et al., 2019; Francis et al., 2015; Legendre et al., 2008; Liu et al., 2019; Pollock et al., 2016; Scheffer et al., 2015; Taylor et al., 2015). The cuticular plate expands postnatally in mouse while stereocilia are still developing (Self et al., 1998; Szarama et al., 2012). Defects in spectrin crosslinkers, LMO7, or rootlet proteins such as ANKRD24, RIPOR2, or TRIOBP cause bundle

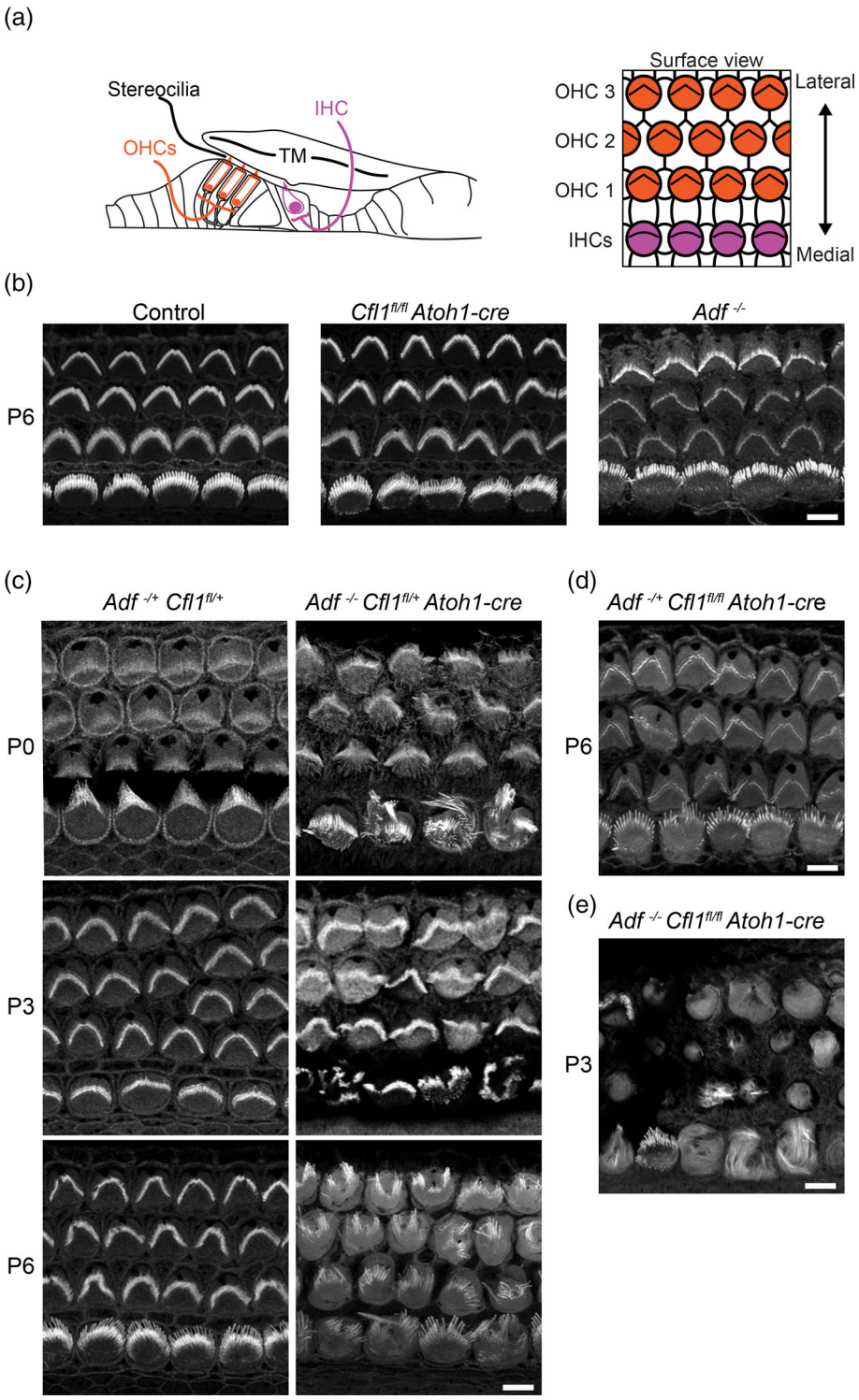

FIGURE 1 Stereocilia bundle shapes of *Adf* and *Cfl1* single and compound mutants. (a) Schematic drawing of cochlear cross-section including inner hair cells (IHCs, purple) and inner hair cells (OHCs, orange). Stereocilia are adjacent to the tectorial membrane. On the right is a diagram of the surface of the organ of Corti showing the arrangement of IHCs and OHCs. (b–d) Surface view of stereocilia bundles labeled with dye-conjugated phalloidin. (b) $Cfl1^{fl/fl}$ controls and $Cfl1^{fl/fl}$ *Atoh1-cre* and $Adf^{-/-}$ mice at P6. (c) $Adf^{-/+}$ $Cfl1^{fl/+}$ littermate control hair cells and the compound mutant $Adf^{-/-}$ $Cfl1^{fl/+}$ *Atoh1-cre* at P0, P3, and P6. (d) $Adf^{-/+}$ $Cfl1^{fl/fl}$ *Atoh1-cre* at P6. (e) $Adf^{-/-}$ $Cfl1^{fl/fl}$ *Atoh1-cre* at P3. All images were taken from the middle turn of cochleae. Scale bars represent 5 μm.

dysmorphology and destabilize stereocilia, leading to their degeneration and hearing loss (Kitajiri et al., 2010; Krey et al., 2022; Zhao et al., 2016), highlighting the functional connection between stereocilia and the cuticular plate.

A third major actin network exists at hair cell junctions, which form coordinately with neighboring support cells. The OHC apical junctions that are formed with neighboring support cells have characteristics of both adherens and tight junctions, providing mechanical strength and preventing transepithelial ion flow (Etournay et al., 2010; Nunes et al., 2006). Constitutively active mDIA1 expression or loss of CDC42 results in dysregulation of IHC and OHC junctions, indicating that proper actin regulation is required for their maintenance (Ninoyu et al., 2020; Ueyama et al., 2014).

We recently identified a role for the actin severing proteins actin depolymerizing factor (ADF, also known as DSTN) and cofilin-1 (CFL1) in regulating F-actin in stereocilia (McGrath et al., 2021). Here,

we investigated how ADF/CFL1 regulates actin in the cuticular plate and at the hair cell junction. ADF and CFL1 are encoded by separate genes but the proteins have very similar biochemical properties (Bamburg, 1999; Wioland et al., 2019). Most notably, ADF/CFL1, which sever F-actin filaments to promote filament disassembly and release actin monomers that can then be rejuvenated to help maintain the G-actin concentration (Pollard & Borisy, 2003). In other contexts, severing produces a new F-actin barbed end that can incorporate monomers and stimulate filament growth (Ghosh et al., 2004). We investigated the effect of ADF/CFL1 activity on the F-actin networks at cell junctions and in the cuticular plate by characterizing mouse hair cells with loss of function mutations in one or both genes.

Mutating both *Adf* and *Cfl1* simultaneously in mice caused abnormal growth and disorganization in the cuticular plate and junctional actin networks, which corresponded to disruption of stereocilia bundle shape. Conditional double knockout of ADF and CFL1 later in development largely spared bundle shape but still resulted in expansion and disorganization of the cuticular plate and junctional actin networks. Finally, cuticular plate and junctional actin also overgrew in adult single mutants. Together, these data show that ADF/CFL1 limit F-actin expansion and facilitate actin organization in the cuticular plate and hair cell junction throughout life, and this is required for normal stereocilia bundle patterning and hair cell maintenance.

2 | RESULTS

2.1 | ADF/CFL1 are required for normal stereocilia bundle patterning

To characterize stereocilia bundle morphology we used fluorescence microscopy to image phalloidin-stained sensory epithelia from control ($Cfl1^{fl/fl}$), *Cfl1* knockout ($Cfl1^{fl/fl}$ *Atoh1-cre*), and *Adf* knockout ($Adf^{-/-}$) mice at P6. In control tissue, stereocilia bundles were patterned normally, forming a distinct V-shape (Figure 1b). $Cfl1^{fl/fl}$ *Atoh1-cre* hair cells, where cre-mediated recombination ablated expression of CFL1 in late embryonic to early postnatal development, were patterned similarly to controls, while some $Adf^{-/-}$ hair cell bundles had an elongated and curling leg of the bundle. The *Adf* phenotype is likely more severe because $Adf^{-/-}$ is a whole-body knockout while the floxed *Cfl1* is deleted in hair cells but not adjacent support cells. In addition, cre-mediated *Cfl1* deletion occurs after E12 with variable timing in different cells, which may result in a milder phenotype (Matei et al., 2005).

ADF and CFL1 show compensatory function in mouse auditory hair cells (McGrath et al., 2021), so we next characterized compound mutants lacking three of the four *Adf/Cfl1* alleles. $Adf^{-/-}$ $Cfl1^{fl/+}$ *Atoh1-cre* mice show a bundle patterning defect that is evident by P0 and more pronounced at P3 and P6 (Figure 1c). The type of dysmorphology varied considerably between hair cells within a single turn of tissue, perhaps reflecting variable timing of transgenic *Atoh1*-cre expression (Matei et al., 2005; Perrin et al., 2010; Tarchini et al., 2016). Instead of the normal V-shape, bundles ranged broadly from nearly normal in shape to flattened or inverted, as well as wavey, splayed, split, swollen, or degenerated. The other compound mutant, $Adf^{-/+}$ $Cfl1^{fl/fl}$ *Atoh1-cre*, showed a similar but less severe phenotype (Figure 1d). Finally, $Adf^{-/-}$ $Cfl1^{fl/fl}$ *Atoh1-cre* double knockouts had the most severe derangement of stereocilia bundles (Figure 1e). Together, these observations show that ADF and CFL1 contribute to the overall organization of stereocilia into V-shaped bundles along the mediolateral axis.

2.2 | Actin accumulates in the cuticular plate and apical junctions of *Adf/Cfl1* mutants

Since stereocilia bundles develop concurrently with the cuticular plate and cell junctions, we assessed the effect of ADF and CFL1 loss on these actin structures. We stained F-actin in each compound mutant and imaged cells by first focusing on the bundles and then on the junctional level, which includes the cuticular plate (Figure 2a). In heterozygous control cells, phalloidin stains a ring of F-actin around the cell as well as the cuticular plate, which is not as bright as the junctional actin (Figure 2b). In contrast, $Adf^{-/-}$ $Cfl1^{fl/+}$ *Atoh1-cre* hair cells had considerably brighter phalloidin staining, marking enlarged junctions and disorganized cuticular plates (Figure 2b). $Adf^{-/-}$ $Cfl1^{fl/fl}$ *Atoh1-cre* double knockout cells had even more prominent F-actin accumulations where the junctional and cuticular plate apparently merge together (Figure 2b). In addition, we noted that bundle morphology was variable within a sample and the more mildly affected bundles generally had F-actin at the junctional level that was more similar to control cells (Figure 2b, arrows). Loss of ADF or CFL1 had similar effects in IHCs and OHCs. Together, these results suggest that ADF/CFL1 activity slows or antagonizes expansion of the cuticular plate and contributes to actin organization, with defects in this process correlating with defects in bundle patterning.

2.3 | The effect of early postnatal ablation of ADF/CFL1 on F-actin structures

To bypass potential effects on early bundle patterning, we used a conditional knockout strategy where tamoxifen was administered to $Adf^{-/-}$ $Cfl1^{fl/fl}$ *Cagg-creER* (inducible double knockout [iDKO]) mice at P2 and hair cells in the middle turn of cochleae were analyzed at P5 by imaging F-actin. $Adf^{-/+}$ $Cfl1^{fl/fl}$ control bundles formed normal V- and U-shaped patterns in OHCs and IHCs, respectively (Figure 3a). The stereocilia bundles of iDKO hair cells appeared only mildly disrupted in comparison to compound mutants (Figures 1 and 3a,b). However, compared with littermate control hair cells, the actin networks comprising the cuticular plate, apical junctions, and the lateral wall in iDKO IHCs and OHCs were often larger with more F-actin (Figure 3b–e). In addition, we also observed long and dense F-actin structures within the cell body (Figure 3b). F-actin was more abundant in the medial and lateral border regions of iDKO IHCs, and

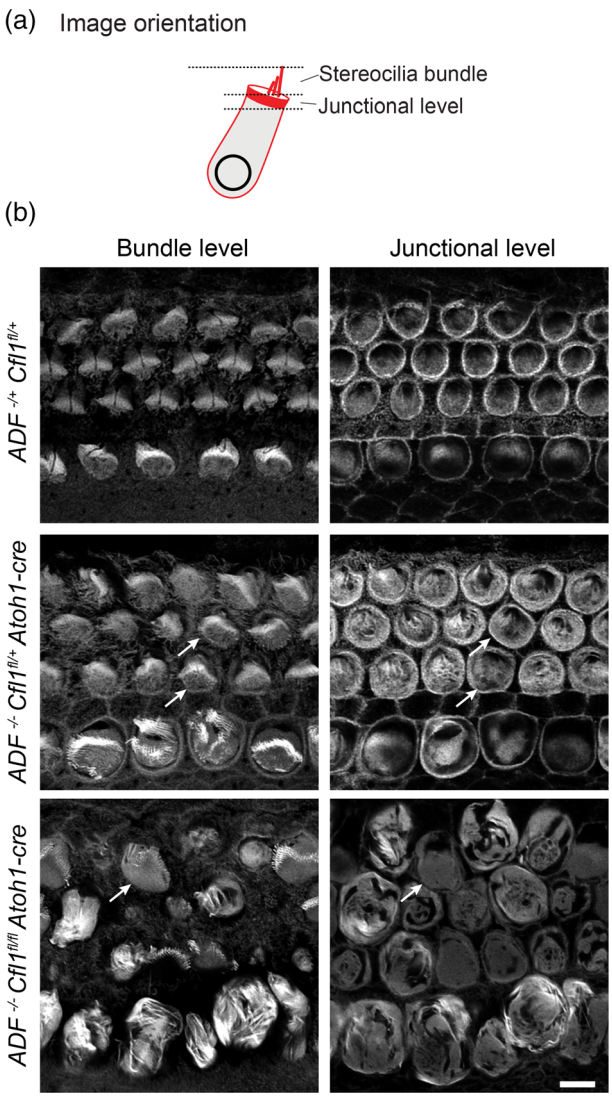

FIGURE 2 Stereocilia bundle dysmorphology of *Adf* and *Cfl1* compound mutants correlates with junctional F-Actin defects. (a) Schematic showing the position of the image slices of hair cells in (b). From top to bottom, $Adf^{-/+}$ $Cfl1^{fl/+}$, $Adf^{-/-}$ $Cfl1^{fl/+}$ *Atoh1-cre*, and $Adf^{-/-}$ $Cfl1^{fl/fl}$ *Atoh1-cre* samples at P0. Bundle-level and junctional-level images are sum image projections from the regions shown in the schematic in (a). Arrows indicate examples with more normal bundle morphology. All images are the same magnification, taken from the middle turn of cochleae, and the scale bar represents 5 μm.

extended down into the cell body, becoming particularly extensive along the lateral wall (Figure 3c). IHCs of iDKO mice had cuticular plates which were sometimes visibly disorganized, forming holes in the medial end of the structure (Figure 3c, arrowhead) and were on average thicker with more F-actin (Figure 3e). OHCs in iDKO mice also had more F-actin around their periphery and cuticular plates that were thicker with more intense phalloidin staining (Figure 3d,e). Together, the phenotypes of the iDKO mutants demonstrate an ongoing postnatal role for ADF/CFL1 in restricting actin network expansion in hair cell cuticular plates and apical junctions even after bundle position and shape have been established.

2.4 | ADF/CFL1 localization is not correlated with dysregulation of apical actins structures

To better understand the role of ADF/CFL1 in the cuticular plate and lateral wall, we immunolocalized these proteins in IHCs and OHCs in iDKO mice. We previously demonstrated that the antibody detects both ADF and CFL1 and that staining is lost in some stereocilia bundles following creER induction, showing the antibody is likely specific for ADF/CFL1 (McGrath et al., 2021). We also found that staining is retained in other hair cell bundles, presumably because inefficient recombination of the *Cfl1-flox* allele. By focusing on the bundles in iDKO hair cells, we identified cells that lost ADF/CFL adjacent to cells that retained ADF/CFL in their stereocilia (Figure 4a). Cells lacking ADF/CFL1 staining in their bundles also had increased F-actin staining in their cuticular plate and perijunctional regions without apparent reduction of ADF/CFL1 levels as gauged by comparison of adjacent cells (Figure 4b). Thus, ADF/CFL1 is a level that cannot be detected above background signal or these proteins may act indirectly on cuticular plate and junctional actin.

2.5 | ADF/CFL1 regulate F-actin in IHC cuticular plate and junctional actin in adult hair cells

To determine if ADF and CFL1 continue to regulate F-actin in mature hair cells, we characterized each single knockout at 4–6 months of age by SEM. OHC stereocilia bundle shape and orientation defects were more evident in $Adf^{-/-}$ mice compared with control C57Bl/6, $Cfl1^{fl/fl}$, or $Adf^{+/-}$, or $Cfl1^{fl/fl}$ *Atoh1*-cre mice (Figure 5a), and were dysmorphic as previously observed (Narayanan et al., 2015). CFL1-deficient OHC stereocilia were more normal in appearance (Figure 5a). In contrast, most $Cfl1^{fl/fl}$ *Atoh1*-cre IHCs were severely affected, having a swollen apical surface with stereocilia fusion. $Adf^{-/-}$ IHCs had a similar, though less severe phenotype, where the medial aspect of the apical surface was swollen. We analyzed the distribution of F-actin in 4- to 6-month-old $Adf^{-/-}$ mice in the cuticular plate and perijunctional region (Figure 5b). Most intriguingly, we noted an accumulation of phalloidin-stained F-actin at the medial edge of the cell, which appears to bridge the cuticular plate and lateral wall actin. These data show that ADF/CFL1 continue to regulate cuticular plate and junctional actin after hair cell maturation has completed, with loss of their activity resulting in F-actin overgrowth.

3 | DISCUSSION

Decreased ADF/CFL1 expression caused increased levels of F-actin in the cuticular plate and perijunctional structures of auditory hair cells. If loss occurred early in development, stereocilia bundles were also mispatterned, suggesting that abnormal F-actin expansion in apical structures distorted developing bundles of constitutive *Adf/Cfl1* mutants. Ablating ADF/CFL1 later in postnatal development largely spared bundle shape but F-actin in the cuticular plate and perijunctional

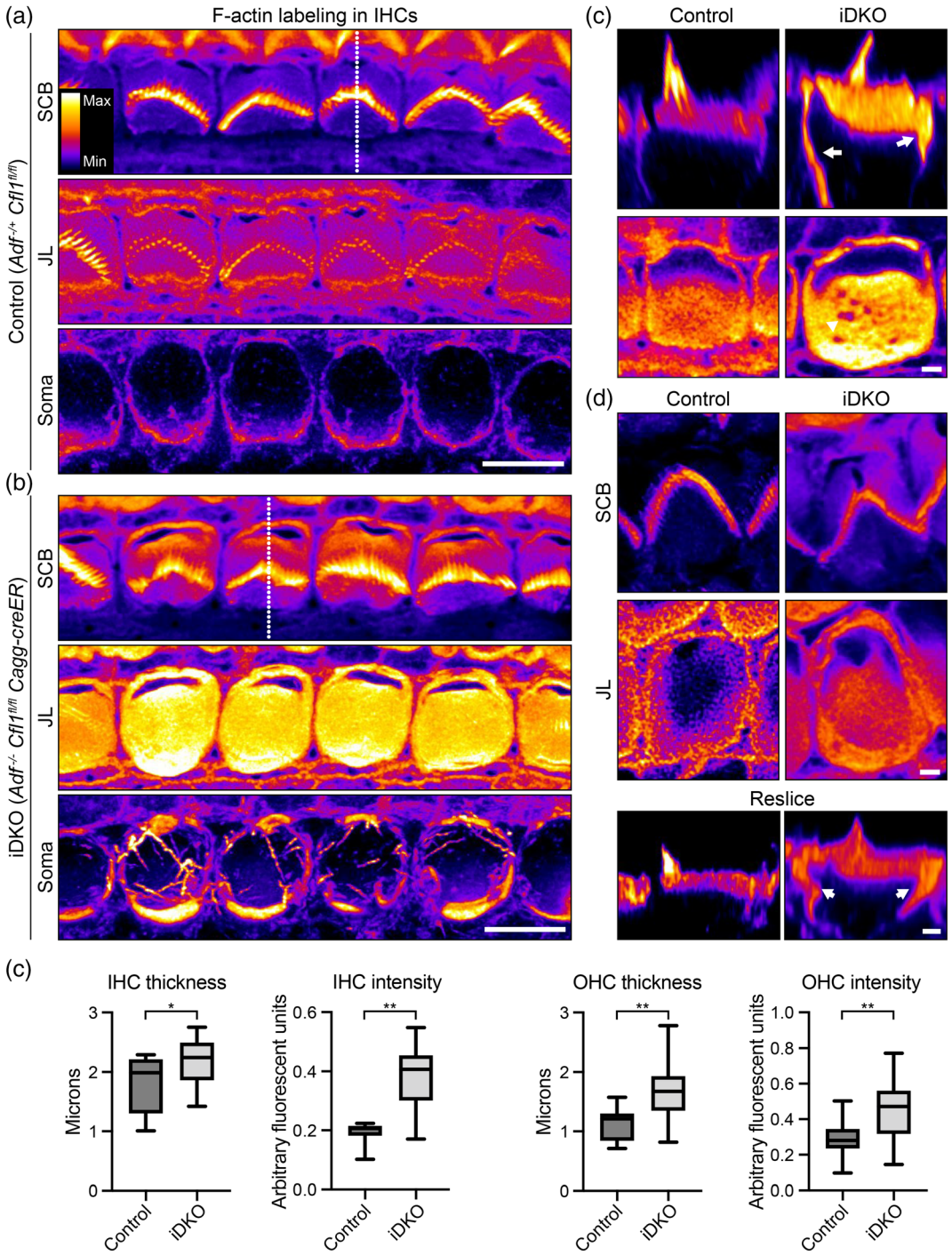

FIGURE 3 F-actin distribution in P5-induced *Adf/Cfl1* double knockouts. *Adf/Cfl1* double knockouts generated by tamoxifen injection of *Adf*$^{-/-}$ *Cfl1*$^{fl/fl}$ *Cagg-creER* mice (inducible double knockout [iDKO]) at P2 and analyzed at P5. F-actin was stained with phalloidin and intensity represented by a heat map look-up-table where max intensity was scaled according to stereocilia. The same scaling was used in other images from the same stack showing other levels of the cell. (a,b) inner hair cell (IHC) images are slices from three focal planes including the stereocilia bundles (SCB), junction level (JL) starting just below the bundle, and the soma starting below the cuticular plate (CP). (a) *Adf*$^{-/+}$ *Cfl1*$^{fl/fl}$ littermate controls and (b) iDKO mice. (c) Digitally reconstructed slices show the z-profile of IHCs from control and iDKO cells, which were generated along white dotted lines in (a,b. Accumulation of F-actin in iDKO IHC lateral walls and junctions indicated by white arrows. Single image plane of iDKO IHC CP showing regions lacking phalloidin labeling (arrowhead). (d) Outer hair cells (OHCs) at stereocilia bundle and junctional levels. The z-reslice was taken at the vertices of bundles shown in the SCB panels. Arrows indicate increased F-actin. Scale bars are 1 μm. (e) Quantification of CP thickness and phalloidin intensity in IHCs and OHCs. *p < 0.001, **p < 0.0001 by Mann–Whitney U test (a,b) Scale bars represent 5 μm. (c,d) Scale bars represent 1 μm. All images were taken from the middle turn of cochleae.

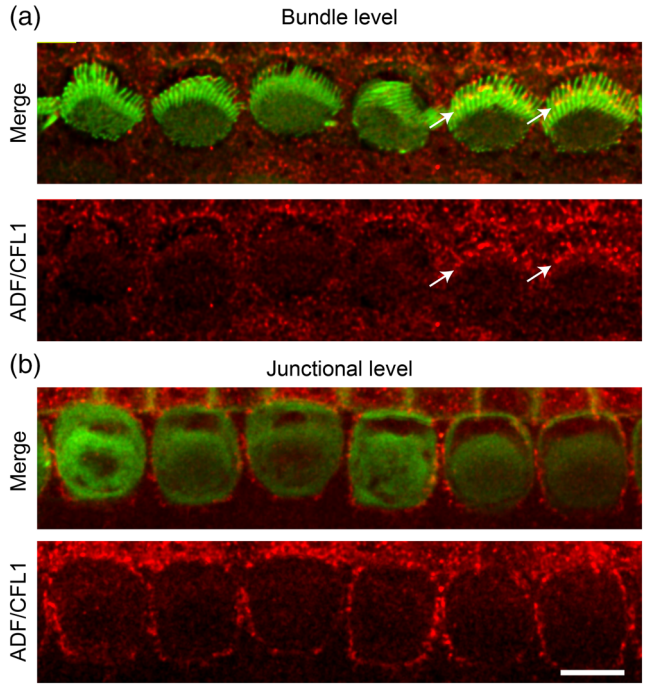

FIGURE 4 Actin depolymerizing factor/cofilin-1 (ADF/CFL1) labeling in inducible double knockouts. Induced double knockout inner house cells at P6 in the middle turn immunolabeled for ADF/CFL1 (red) and β-actin (green). (a) Bundle level maximum intensity image projections show ADF/CFL1 in stereocilia from the two right-most cells (arrows) but missing from the remaining bundles. (b) Junctional-level maximum intensity image projections show little ADF/CFL1 labeling near the cuticular plate. More intense staining at the periphery is similar and may be outside the cell. Scale bar represents 5 μm. All images were taken from the middle turn of cochleae.

regions continued to expand. Regulation of these actin structures continues in adult cells because loss of either ADF or CFL1 alone, which initially caused only minor defects, eventually resulted in increased F-actin in IHC apical regions that correlated with a bulging apical surface and stereocilia fusion. Together, these data show that actin disassembling proteins ADF and CFL1 regulate F-actin in the cuticular plate and near cell contacts of auditory hair cells.

ADF and CFL1 partially compensate for the loss of the other and the most evident phenotypes including bundle shape defects and F-actin accumulation in the cuticular plate and perijunctional structures are more penetrant in compound mutants. These phenotypes suggest that ADF and CFL1 protein levels collectively need to be high enough to effectively remove F-actin, likely through their severing and/or depolymerizing activities. Without disassembly, apical actin structures continue to expand even in adult cells. The resulting phenotypes resemble those seen when the formins mDIA1 and 3 were overexpressed (Ninoyu et al., 2020; Schoen et al., 2013), as well as *CapZβ Atoh1-cre* conditional knockouts (Avenarius et al., 2017). Therefore, the balance of F-actin assembly and disassembly is important for maintaining the size and organization of the cuticular plate.

Interestingly, ADF/CFL1 immunostaining in the cuticular plate or perijunctional region was near background levels. In addition, the signal did not diminish in induced double knockout cells that developed evident and abnormal F-actin accumulations. In contrast, ADF/CFL1 staining in the stereocilia bundle was clearly lost in the most affected cells, implying that antibody staining was specific. This may mean that ADF and CFL1, which are small, cytoplasmic proteins, regulate cuticular plate and perijunctional F-actin without robustly localizing to those structures. For example, the proteins could transiently associate with the edges of the cuticular plate or localize diffusely without accumulating to a level detectable by our staining protocol. Alternatively, ADF/CFL1 could regulate the cellular levels of G-actin in a way that indirectly impacts actin-based structures.

When ADF and CFL1 were ablated after P2, bundle shape was largely maintained but the cuticular plate and perijunctional F-actin populations expanded. ADF and CFL1 continue to regulate these structures in mature hair cells, which became dysmorphic in *Adf* and *Cfl1* single knockouts. These data show that perijunctional and cuticular plate actin populations require active maintenance to preserve hair cell integrity and function as mice age.

4 | MATERIALS AND METHODS

4.1 | Mouse models

All mouse lines have been previously described. The transgenes used drive tissue-specific Cre recombinase expression in this study include *Atoh1-cre* (MGI:3775845, Matei et al., 2005) and *Cagg-creER* (MGI:2182767, JAX:004682) mouse lines. The $Adf^{-/-}$ ($Dstn^{corn1/corn1}$, MGI: 1889311, Ikeda et al., 2003) mice were generously provided by the Ikeda lab (University of Wisconsin-Madison) and $Cfl1^{fl/fl}$ ($Cfl1^{tm1.1Wit}$, MGI:4943295, Gurniak et al., 2005) mice were graciously provided by Walter Witke and Christine Gurniak (University of Bonn). Mice used in this study were backcrossed to and maintained on a C57BL/6 background.

4.2 | Scanning electron microscopy

Cochlear tissue was prepared for and examined by scanning electron microscopy (SEM). Dissected tissue was fixed in 2.5% glutaraldehyde, 0.1 M sodium cacodylate supplemented with 2 mM $CaCl_2$ for 4 h at room temperature or 16–18 h at 4°C. To reduce surface charging, the tissue was incubated in 2% each of arginine, glutamine, glycine, and sucrose in water for 16–18 h, then in 2% tannic acid and guanidine hydrochloride in water for 2 h, followed by incubation in 1% OsO_4 in water for 1 h. Samples were washed three times with water in between solutions. The samples were afterward transitioned to 100% ethanol, then transitioned to CO_2 and desiccated using a Tousimis Research Corporation Samdri-780 critical point dryer. Samples

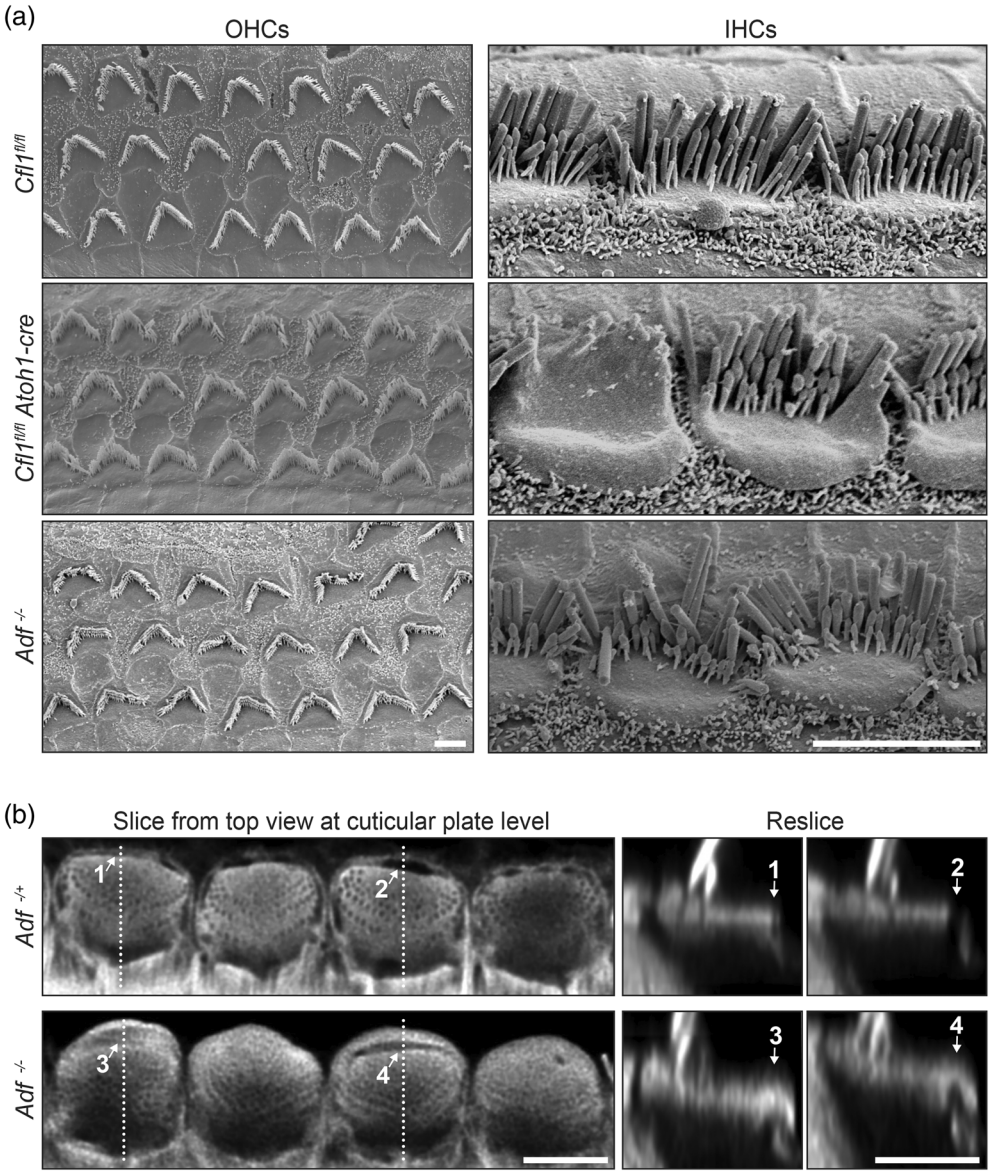

FIGURE 5 Phenotypes in adult *Adf* or *Cfl1* knockout hair cells. $Adf^{-/-}$ and $Cfl1^{fl/fl}$ *Atoh1-cre* knockout mice at 4–6 months of age. (a) Scanning electron micrographs of the organ of Corti apical surface showing outer house cell (OHC) and inner house cell (IHC) stereocilia bundles. (b) F-actin in $Adf^{-/+}$ and $Adf^{-/-}$ IHCs were stained with phalloidin to reveal the cuticular plates of $Adf^{-/+}$ and $Adf^{-/-}$ hair cells. Z-resliced images were generated along the dotted white lines. The numbered arrows indicate corresponding locations in the top view and where the cuticular plate and perijunctional region are connected by F-actin in $Adf^{-/-}$ cells. Scale bars represent 5 μm. All images were taken from the middle turn of cochleae.

were sputter coated with gold before imaging with a JEOL JSM-7800F Schottky field emission scanning electron microscope.

4.3 | Immunofluorescence microscopy

The cochlear shell was removed from the temporal bone and placed in phosphate-buffered saline (PBS). The bone and excess tissue surrounding the organ of Corti were removed to expose the sensory epithelium. The tectorial membranwas removed after fixation. Dissected tissue was fixed in 4% paraformaldehyde in PBS for 16–18 h at 4°C. To label ADF and CFL1, the middle turn was dissected, then placed in 100% methanol for 10 min at −20°C, followed by permeabilization with 0.5% Triton X-100 (Sigma, Cat. no. X-100-100ML) in PBS for 10 min at room temperature, and blocked with 5% goat serum (Sigma, Cat. no. G9023-10ML) in PBS for 2 or 16–18 h at 4°C. Samples were then stained with 1:100 dilution of anti-CFL1 rabbit monoclonal antibody (Cell Signaling Technology, Cat. no. 5175, 52.0 μg/mL) and 1:400 dilution of anti-β-actin mouse monoclonal antibody conjugated to a FITC dye (Abcam, Cat. no. ab6277, 2.9 mg/mL) in 5% goat serum for 1 h. Unlabeled primary antibodies were detected using either Alexa-488 (Invitrogen, Cat. no. A11029, 2 mg/mL), Alexa-546 (Invitrogen, Cat. no. A11035, 2 mg/mL), or Alexa-568 (Invitrogen, Cat. no. A11036, 2 mg/mL). Actin in nonmethanol treated samples was stained with 1:400 phalloidin labeled with Alexa-488 (Invitrogen, Cat. no. A12379), Alexa-568 (Invitrogen, Cat. no. A12380), or Alexa-647 (Invitrogen, Cat. no. A22287) in 5% goat serum. Three washes with PBS were done for each change between incubation solutions. Samples were mounted in Prolong Diamond (Fisher Scientific, P36961), cured overnight in the dark, and imaged with a Leica Plan Apo 63X NA 1.40 oil immersion objective on Leica SP8 inverted confocal microscope operating in resonant mode. Images were captured using Leica Application Suite X and deconvolved using Leica LIGHTNING deconvolution with the recommended settings.

4.4 | Quantification of cuticular plate thickness and intensity

A custom MATLAB script was used to measure cuticular plate thickness and F-actin labeling intensity relative to that of the stereocilia bundle. The MATLAB code is annotated and freely available on GitHub (https://github.com/mcgrathjk/McGrath2022_CP_analysis). Communications to the author can be done through this information portal. In brief, a rectangular region of interest (ROI) over the bundle and a line perpendicular to the cuticular plate were drawn on projections generated from the image stack, which were then used to analyze each image in the stack. Each image in the stack was analyzed separately and averaged to obtain the reported measures. The edges of the cuticular plate were defined as the first pixels to reach 70% of the most frequent non-zero pixel value on each side of the cuticular plate. The distance between the edges determined this way was used to define the thickness of the cuticular plate. Pixel values between the defined edges along the line selection were averaged to determine the intensity value reported for cuticular plate. Intensity values were normalized to the average top 5% of pixel intensity values of the stereocilia bundle ROI.

AUTHOR CONTRIBUTIONS

J.M. and B.J.P. conceived the study, designed the experiments, and analyzed the data. J.M. and K.H performed the experiments. All authors contributed to writing the article.

FUNDING INFORMATION

U.S. Department of Health and Human Services, National Institutes of Health.

CONFLICT OF INTEREST STATEMENT

The authors declare no conflicts of interest.

DATA AVAILABILITY STATEMENT

The data that support the findings of this study are available from the corresponding author upon reasonable request.

REFERENCES

Avenarius, M. R., Krey, J. F., Dumont, R. A., Morgan, C. P., Benson, C. B., Vijayakumar, S., Cunningham, C. L., Scheffer, D. I., Corey, D. P., Muller, U., Jones, S. M., & Barr-Gillespie, P. G. (2017). Heterodimeric capping protein is required for stereocilia length and width regulation. *The Journal of Cell Biology*, *216*, 3861–3881.

Bamburg, J. R. (1999). Proteins of the ADF/cofilin family: Essential regulators of actin dynamics. *Annual Review of Cell and Developmental Biology*, *15*, 185–230.

Du, T. T., Dewey, J. B., Wagner, E. L., Cui, R., Heo, J., Park, J. J., Francis, S. P., Perez-Reyes, E., Guillot, S. J., Sherman, N. E., Xu, W., Oghalai, J. S., Kachar, B., & Shin, J. B. (2019). LMO7 deficiency reveals the significance of the cuticular plate for hearing function. *Nature Communications*, *10*, 1117.

Etournay, R., Lepelletier, L., Boutet de Monvel, J., Michel, V., Cayet, N., Leibovici, M., Weil, D., Foucher, I., Hardelin, J. P., & Petit, C. (2010). Cochlear outer hair cells undergo an apical circumference remodeling constrained by the hair bundle shape. *Development*, *137*, 1373–1383.

Francis, S. P., Krey, J. F., Krystofiak, E. S., Cui, R., Nanda, S., Xu, W., Kachar, B., Barr-Gillespie, P. G., & Shin, J. B. (2015). A short splice form of Xin-actin binding repeat containing 2 (XIRP2) lacking the Xin repeats is required for maintenance of stereocilia morphology and hearing function. *The Journal of Neuroscience*, *35*, 1999–2014.

Ghosh, M., Song, X., Mouneimne, G., Sidani, M., Lawrence, D. S., & Condeelis, J. S. (2004). Cofilin promotes actin polymerization and defines the direction of cell motility. *Science*, *304*, 743–746.

Gurniak, C. B., Perlas, E., & Witke, W. (2005). The actin depolymerizing factor n-cofilin is essential for neural tube morphogenesis and neural crest cell migration. *Developmental Biology*, *278*, 231–241.

Ikeda, S., Cunningham, L. A., Boggess, D., Hawes, N., Hobson, C. D., Sundberg, J. P., Naggert, J. K., Smith, R. S., & Nishina, P. M. (2003). Aberrant actin cytoskeleton leads to accelerated proliferation of corneal epithelial cells in mice deficient for destrin (actin depolymerizing factor). *Human Molecular Genetics*, *12*, 1029–1037.

Kitajiri, S., Sakamoto, T., Belyantseva, I. A., Goodyear, R. J., Stepanyan, R., Fujiwara, I., Bird, J. E., Riazuddin, S., Riazuddin, S., Ahmed, Z. M., Hinshaw, J. E., Sellers, J., Bartles, J. R., Hammer, J. A., 3rd, Richardson, G. P., Griffith, A. J., Frolenkov, G. I., & Friedman, T. B. (2010). Actin-bundling protein TRIOBP forms resilient rootlets of hair cell stereocilia essential for hearing. *Cell*, *141*, 786–798.

Krey, J. F., Liu, C., Belyantseva, I. A., Bateschell, M., Dumont, R. A., Goldsmith, J., Chatterjee, P., Morrill, R. S., Fedorov, L. M., Foster, S., Kim, J., Nuttall, A. L., Jones, S. M., Choi, D., Friedman, T. B., Ricci, A. J., Zhao, B., & Barr-Gillespie, P. G. (2022). ANKRD24 organizes TRIOBP to reinforce stereocilia insertion points. *The Journal of Cell Biology*, *221*, e202109134.

Legendre, K., Safieddine, S., Kussel-Andermann, P., Petit, C., & El-Amraoui, A. (2008). alphaII-betaV spectrin bridges the plasma membrane and cortical lattice in the lateral wall of the auditory outer hair cells. *Journal of Cell Science*, *121*, 3347–3356.

Liu, Y., Qi, J., Chen, X., Tang, M., Chu, C., Zhu, W., Li, H., Tian, C., Yang, G., Zhong, C., Zhang, Y., Ni, G., He, S., Chai, R., & Zhong, G. (2019). Critical role of spectrin in hearing development and deafness. *Science Advances*, *5*, eaav7803.

Matei, V., Pauley, S., Kaing, S., Rowitch, D., Beisel, K. W., Morris, K., Feng, F., Jones, K., Lee, J., & Fritzsch, B. (2005). Smaller inner ear sensory epithelia in Neurog 1 null mice are related to earlier hair cell cycle exit. *Developmental Dynamics*, *234*, 633–650.

McGrath, J., Tung, C. Y., Liao, X., Belyantseva, I. A., Roy, P., Chakraborty, O., Li, J., Berbari, N. F., Faaborg-Andersen, C. C., Barzik, M., Bird, J. E., Zhao, B., Balakrishnan, L., Friedman, T. B., & Perrin, B. J. (2021). Actin at stereocilia tips is regulated by mechanotransduction and ADF/cofilin. *Current Biology*, *31*(1141-53), e7.

Narayanan, P., Chatterton, P., Ikeda, A., Ikeda, S., Corey, D. P., Ervasti, J. M., & Perrin, B. J. (2015). Length regulation of mechanosensitive stereocilia depends on very slow actin dynamics and filament-severing proteins. *Nature Communications*, *6*, 6855.

Ninoyu, Y., Sakaguchi, H., Lin, C., Suzuki, T., Hirano, S., Hisa, Y., Saito, N., & Ueyama, T. (2020). The integrity of cochlear hair cells is established and maintained through the localization of Dia1 at apical junctional complexes and stereocilia. *Cell Death & Disease*, *11*, 536.

Nunes, F. D., Lopez, L. N., Lin, H. W., Davies, C., Azevedo, R. B., Gow, A., & Kachar, B. (2006). Distinct subdomain organization and molecular composition of a tight junction with adherens junction features. *Journal of Cell Science*, *119*, 4819–4827.

Perrin, B. J., Sonnemann, K. J., & Ervasti, J. M. (2010). Beta-actin and gamma-actin are each dispensable for auditory hair cell development but required for stereocilia maintenance. *PLoS Genetics*, *6*, e1001158.

Pollard, T. D., & Borisy, G. G. (2003). Cellular motility driven by assembly and disassembly of actin filaments. *Cell*, *112*, 453–465.

Pollock, L. M., Gupta, N., Chen, X., Luna, E. J., & McDermott, B. M., Jr. (2016). Supervillin is a component of the hair cell's cuticular plate and

the head plates of organ of Corti supporting cells. *PLoS One*, *11*, e0158349.

Scheffer, D. I., Zhang, D. S., Shen, J., Indzhykulian, A., Karavitaki, K. D., Xu, Y. J., Wang, Q., Lin, J. J., Chen, Z. Y., & Corey, D. P. (2015). XIRP2, an actin-binding protein essential for inner ear hair-cell stereocilia. *Cell Reports*, *10*, 1811–1818.

Schoen, C. J., Burmeister, M., & Lesperance, M. M. (2013). Diaphanous homolog 3 (Diap3) overexpression causes progressive hearing loss and inner hair cell defects in a transgenic mouse model of human deafness. *PLoS One*, *8*, e56520.

Self, T., Mahony, M., Fleming, J., Walsh, J., Brown, S. D., & Steel, K. P. (1998). Shaker-1 mutations reveal roles for myosin VIIA in both development and function of cochlear hair cells. *Development*, *125*, 557–566.

Szarama, K. B., Gavara, N., Petralia, R. S., Kelley, M. W., & Chadwick, R. S. (2012). Cytoskeletal changes in actin and microtubules underlie the developing surface mechanical properties of sensory and supporting cells in the mouse cochlea. *Development*, *139*, 2187–2197.

Tarchini, B., Tadenev, A. L., Devanney, N., & Cayouette, M. (2016). A link between planar polarity and staircase-like bundle architecture in hair cells. *Development*, *143*, 3926–3932.

Taylor, R., Bullen, A., Johnson, S. L., Grimm-Gunter, E. M., Rivero, F., Marcotti, W., Forge, A., & Daudet, N. (2015). Absence of plastin 1 causes abnormal maintenance of hair cell stereocilia and a moderate form of hearing loss in mice. *Human Molecular Genetics*, *24*, 37–49.

Tilney, L. G., Derosier, D. J., & Mulroy, M. J. (1980). The organization of actin filaments in the stereocilia of cochlear hair cells. *The Journal of Cell Biology*, *86*, 244–259.

Ueyama, T., Sakaguchi, H., Nakamura, T., Goto, A., Morioka, S., Shimizu, A., Nakao, K., Hishikawa, Y., Ninoyu, Y., Kassai, H., Suetsugu, S., Koji, T., Fritzsch, B., Yonemura, S., Hisa, Y., Matsuda, M., Aiba, A., & Saito, N. (2014). Maintenance of stereocilia and apical junctional complexes by Cdc42 in cochlear hair cells. *Journal of Cell Science*, *127*, 2040–2052.

Wioland, H., Jegou, A., & Romet-Lemonne, G. (2019). Quantitative variations with pH of actin depolymerizing factor/Cofilin's multiple actions on actin filaments. *Biochemistry*, *58*, 40–47.

Zhao, B., Wu, Z., & Muller, U. (2016). Murine Fam65b forms ring-like structures at the base of stereocilia critical for mechanosensory hair cell function. *eLife*, *5*, e14222.

How to cite this article: McGrath, J., Hawbaker, K., & Perrin, B. J. (2025). F-actin in the cuticular plate and junctions of auditory hair cells is regulated by ADF and cofilin to allow for normal stereocilia bundle patterning and maintenance. *Cytoskeleton*, *82*(5), 302–310. https://doi.org/10.1002/cm.21933